

## MISO Measurements in Indoor Environments at 25 GHz

Mohamed Abdulali, Amar Al-Jzari and Sana Salous

Centre for Communications Systems, Department of Engineering, Durham University, Durham, UK, DH1 3LE  
Sana.salous@durham.ac.uk

### Abstract

This paper presents the results of parameter measurements in two indoor environments for both line of sight (LoS) and non-line of sight (NLoS) scenarios at 25 GHz using multiple directional antennae at the transmitter and a single omnidirectional antenna at the receiver (MISO) with the custom-designed channel sounder developed at Durham University. The data are analysed to estimate the K-factor, path loss parameters and root mean square (RMS) delay spread for each scenario. The 50% and 90% values of the RMS delay spread values for a 20 dB threshold are presented for both scenarios.

### 1 Introduction

In indoor wireless communication environments, the received signal is comprised of different MPCs, due to diffraction, reflection or scattering, depending on the environment. This paper presents a description of measurements using a circular array of 8 directional antennae at the transmitter and an omnidirectional antenna at the receiver in a corridor and an office environment with desks and computers in both LoS and NLoS scenarios centred at 25 GHz which is one of the frequency bands identified in the World Radiocommunications Conference in 2019 (WRC19) for 5G networks.

Several parameters have been estimated from the measurements to characterise the channel parameters which include the Rician K-factor, path loss and RMS delay spread.

### 2 Measurement

The measurements were performed using the chirp or frequency-modulated continuous wave (FMCW) channel sounder, developed at Durham University, [1] with new RF heads operating in the 24.5-30 GHz band with a maximum bandwidth of 3 GHz. The transmitter RF head used in the current measurements consists of 8 transmitters feeding an antenna array of eight directional antennas mounted on a circle to provide full coverage in azimuth. An eight-way switch is deployed to transmit sequentially with a gap to identify the sequence of transmission at the receiver. The RF heads at the receiver consisted of a single receiver with an omni-directional antenna. Table 1. gives the parameters of the measurements where the transmitted signal covered the full 3 GHz bandwidth with the analysis bandwidth of 1 GHz. Two scenarios were measured in a LoS and NLoS set

up which represent a typical corridor and an office environment, as shown in Figure 1.

Table 1. Measurement set-up parameters.

|                        |                 |
|------------------------|-----------------|
| Frequency range (GHz)  | 24.9–27.9       |
| Analysis BW            | (24.9-25.9 GHz) |
| Sweep rate (kHz)       | 1.22            |
| Sampling rate (MHz)    | 40              |
| Link polarization      | VV              |
| Antenna configuration  | 8 by 1          |
| Rx antenna             | Omni            |
| Tx antenna             | 8 directional   |
| Nominal 3 dB beamwidth | 45°             |
| Tx antenna height      | 2.4 m           |
| Rx antenna height      | 1.65 m          |

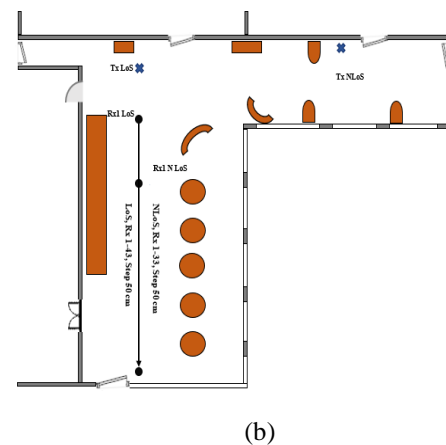
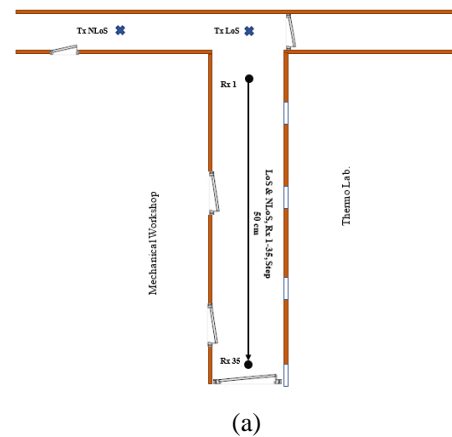
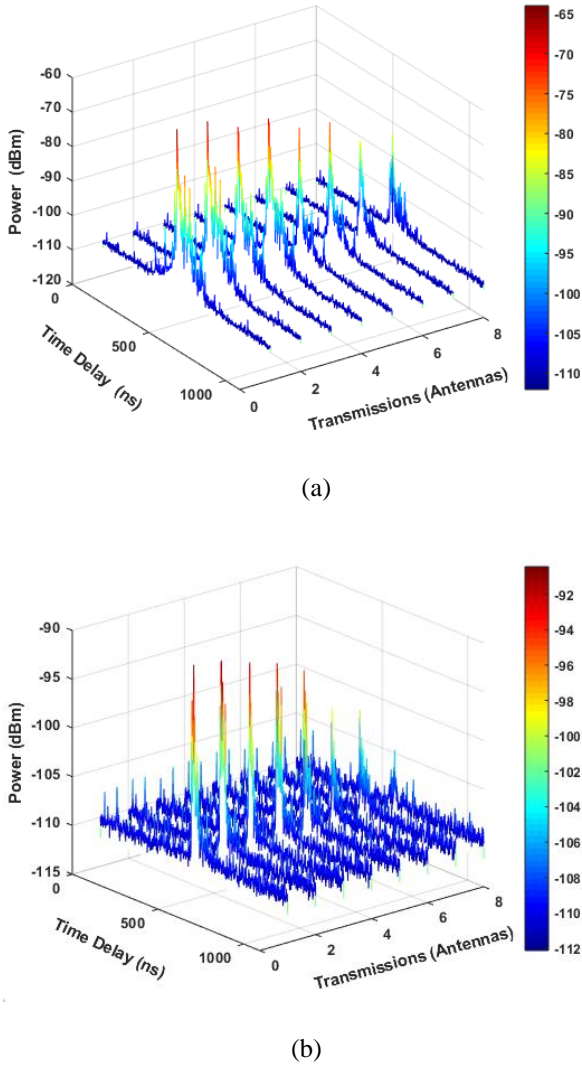


Figure 1. Layout of measurements: (a) corridor, (b) office.

### 3 Measurement analysis

At each location, the omnidirectional antenna receives 8 signals from the 8 transmitters antennas periodically over one second, then the data were processed to estimate 8 power delay profiles (PDPs) for each location as shown in figure 2. Since the transmitter is a circular array of 8 directional antennas, In LoS scenario only one antenna has met the condition of the line of sight with the receiver while the other 7 antennas considered as obstructed line of sight. In the NLoS scenario, there is no antenna of 8 transmitters that has a line of sight with the receiver



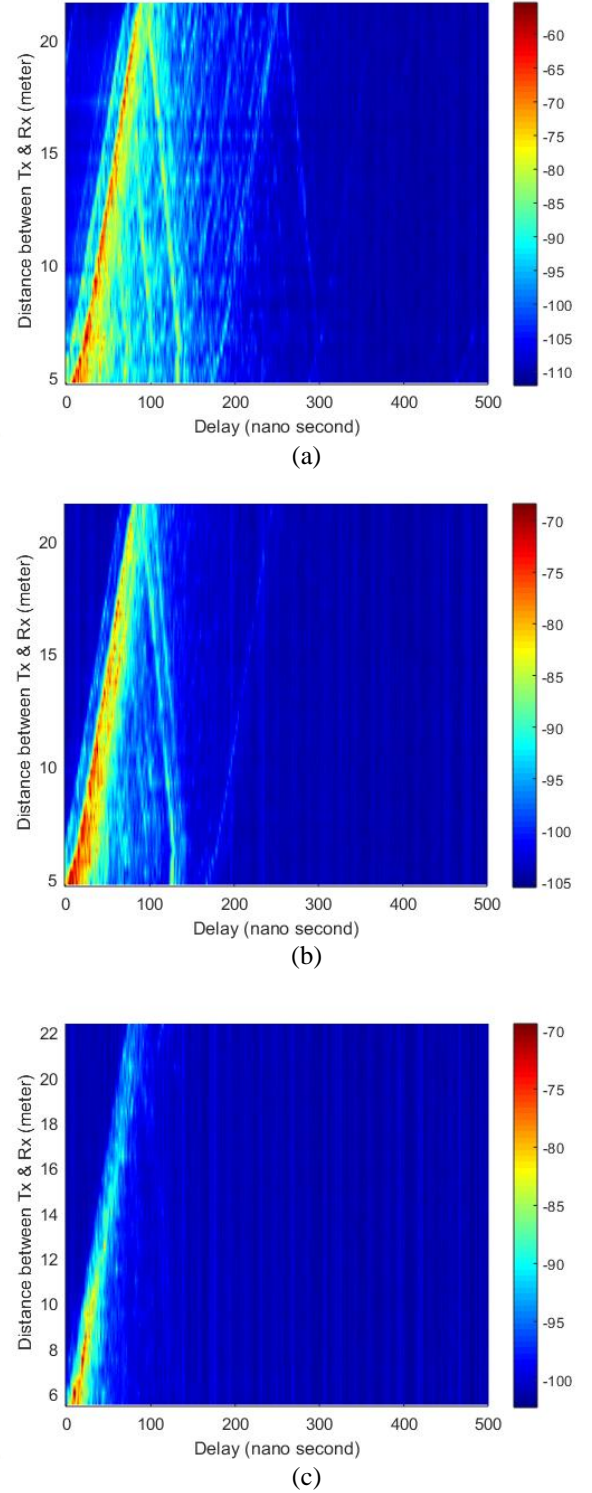
**Figure 2.** The received signals from 8 antennas corridor environment at location no 23: (a) LoS, (b) NLoS.

Figure 3 illustrates the PDPs in the corridor environment for the LoS, OLoS and the NLoS scenarios versus the 3D distance, taking into account the height of the transmitter and the receiver antennas. The LoS gives the strongest PDP of the 8 PDPs at each location while the other 7 PDPs were synthesised to create the OLoS scenario, the synthesis methodology which was utilised is firstly to convert the

PDPs into normal scale and then apply equations 1 and 2, while in NLoS all 8 PDPs were synthesised [2-3].

$$PDP_{syn} = \sum_{i=1}^n PDP_i \quad (1)$$

$$PDP(dB)_{syn} = 10 \log_{10} (PDP_{syn}) \quad (2)$$



**Figure 3.** PDP vs location for the corridor environment: (a) LoS, (b) OLoS and (c) NLoS.

The PDPs were then used to estimate the rms delay spread for 20 dB using equation 3 [4]

$$\tau_{rms} = \sqrt{\frac{\sum_{i=1}^N P_i \tau_i^2}{\sum_{i=1}^N P_i} - \frac{(\sum_{i=1}^N P_i \tau_i)^2}{(\sum_{i=1}^N P_i)^2}} \quad (3)$$

Following calibration, the path loss was estimated using two models: the close-in path loss model, and the floating intercept path loss model, given by equations 4 and 5 respectively [5].

$$PL_{logD} = L(d_0) + N \log_{10} \left( \frac{d}{d_0} \right) + L_f(n) \text{ dB} \quad (4)$$

where  $d_0$  is 1 m and  $L(d_0)$  is the corresponding free-space loss.

$$PL_{logD} = 10\alpha \log_{10}(d) + \beta \text{ dB} \quad (5)$$

where both the distance coefficient  $\alpha$  and the intercept coefficient  $\beta$  are estimated from the measurements.

The data were also analyzed to estimate the fading of the channel versus distance by estimating the K-factor using the method of moments. Since the measurements were performed stationary over one second the K factor was estimated from the instantaneous frequency transfer function  $Hi$  as in equations 6-11 [6] and then taking the one second average.

$$G2 = \frac{1}{n} \sum_{i=1}^n |Hi|^2 \quad (6)$$

$$G4 = \frac{1}{n} \sum_{i=1}^n |Hi|^4 \quad (7)$$

$$S = \sqrt[4]{(2 * G2^2 - G4)} \quad (8)$$

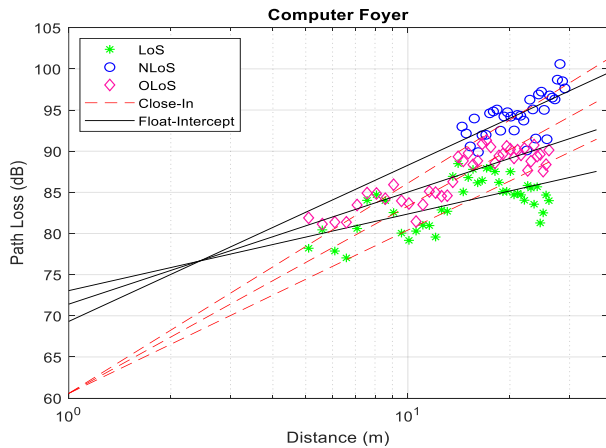
$$\text{Sigma} = \frac{G2 - S^2}{2} \quad (9)$$

$$K = \frac{S^2}{2 * \text{Sigma}} \quad (10)$$

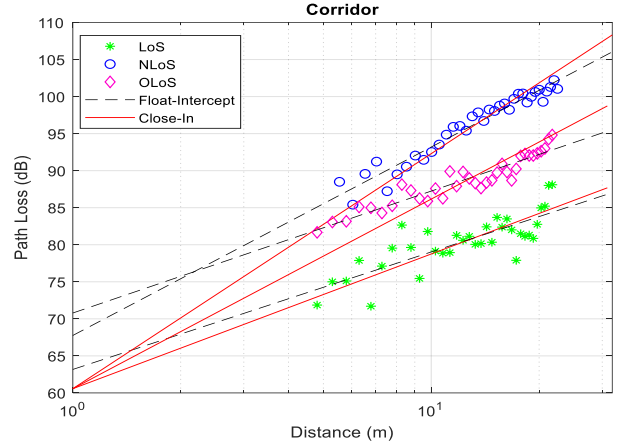
$$K(\text{dB}) = 10 \log_{10}(K) \quad (11)$$

## 4 Estimated channel parameters Results

Figure 4 displays the estimated path loss from the computer foyer and the corridor for both the close-in and the floating intercept models and Table 2 summarises the values of the estimated path loss parameters.



(a)



(b)

Figure 4. Path loss: (a) foyer, (b) corridor.

Table 2. Path loss parameters for the CI and FI models for LoS and NLoS (corridor & computer foyer).

|                                        | Corridor            | Computer Foyer      |
|----------------------------------------|---------------------|---------------------|
| CI/LoS<br>( $\alpha, \sigma$ )         | (1.80, 2.25)        | (1.98, 3.14)        |
| CI/OLoS<br>( $\alpha, \sigma$ )        | (2.55, 2.11)        | (2.27, 2.39)        |
| CI/NLoS<br>( $\alpha, \sigma$ )        | (3.17, 1.54)        | (2.55, 1.98)        |
| FI/LoS<br>( $\alpha, \beta, \sigma$ )  | (1.58, 64.17, 2.17) | (0.93, 73.06, 2.35) |
| FI/OLoS<br>( $\alpha, \beta, \sigma$ ) | (1.64, 70.78, 1.07) | (1.36, 71.41, 1.56) |
| FI/NLoS<br>( $\alpha, \beta, \sigma$ ) | (2.54, 67.75, 1.09) | (1.89, 69.32, 1.89) |

The tables indicates that the close-in model has a higher standard deviation than the floating intercept as it takes free space path loss at 1 meter as a reference, regardless of the type and size of the environment. In the NLoS scenarios, the material of the walls and objects that block the line of sight have significant impact on the path loss. Therefore, the floating intercept data might be more suitable for an indoor path loss estimation.

Figure 5. displays the linear fit of the K-factor for both environments, the corridor and the office for LoS scenario.

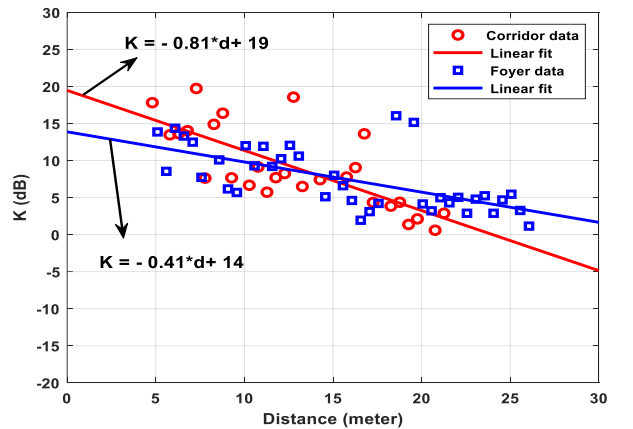


Figure 5. K-factor vs distance LoS.

In the LoS scenario, the K-factor is seen to be inversely proportional to distance which is due to the increased loss of the LoS component which is subject to free-space path loss with distance while the reflected components comparatively increased. the K-factor decreased as the distance increased.

Figure 6 illustrates the cumulative distribution function (CDF) of the RMS delay spread with a summary of the 50% and the 90% values given in Table 3 for the LoS, OLoS and NLoS scenarios for both environments. For each environment, the RMS delay spread results showed that the lowest values are in the LoS scenario where the dominant LoS component was significantly stronger than the scattered and reflected components leading to a smaller delay spread value than the OLoS and NLoS cases. For the corridor environment the OLoS case gave smaller values of delay spread than the NLoS whereas in the open Foyer environment the values were comparable.

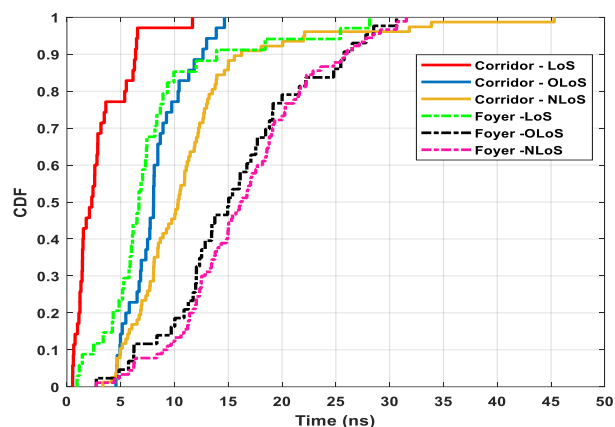


Figure 6. RMS delay spread.

Table 3. RMS delay spread values.

|                    | Corridor       | Computer Foyer |
|--------------------|----------------|----------------|
| LoS<br>(50%, 90%)  | (2.31, 6.38)   | (6.69, 13.91)  |
| OLoS<br>(50%, 90%) | (8.05, 12.64)  | (15.03, 26.04) |
| NLoS<br>(50%, 90%) | (10.30, 16.25) | (16.10, 26.04) |

## 5 Conclusions

Measurements at 25 GHz were conducted in two environments using an 8 transmit by 1 receive antenna configuration in LoS and NLoS scenarios. The LoS measurements were classified as LoS which represent the strongest received signal from the 8 transmit antennas, OLoS which represent the received signal from the remaining 7 antennas which were not in the direct LoS of the receiver. In the NLoS measurements, the received signal from the 8 transmit antennas were combined to

synthesise the PDP. The data were processed to estimate the path loss parameters using the CI and FI models, the Rician K-factor, and the RMS delay spread. The relationship between distance and the K-factor is found to be linear with a higher slope for Corridor than Foyer.

The path loss results indicate that both CI model has a higher standard deviation than the FI model indicating that the FI is more appropriate for the modelling of path loss in indoor environments.

The RMS delay spread results show that the values are directly proportional to the size of the environment.

## 7 References

1. S. Salous, S. M. Feeney, X. Raimundo and A. A. Cheema, "Wideband MIMO Channel Sounder for Radio Measurements in the 60 GHz Band," in IEEE Transactions on Wireless Communications, vol. 15, no. 4, pp. 2825-2832, April 2016.
2. K. Haneda, J. Järveläinen, A. Karttunen, M. Kyrö and J. Putkonen, "A Statistical Spatio-Temporal Radio Channel Model for Large Indoor Environments at 60 and 70 GHz," in IEEE Transactions on Antennas and Propagation, vol. 63, no. 6, pp. 2694-2704, June 2015.
3. A. Bamba, F. Mani and R. D'Errico, "A comparison of indoor channel properties in V and E bands," 2017 11th European Conference on Antennas and Propagation (EUCAP), Paris, 2017.
4. X. Raimundo, S. El-Faitori, Y. Cao and S. Salous, "Outdoor directional radio propagation measurements in the V-band," 2018 IEEE 29th Annual International Symposium on Personal, Indoor and Mobile Radio Communications (PIMRC), Bologna, 2018.
5. X. Raimundo, S. El-Faitori and S. Salous, "Multi-band outdoor measurements in a residential environment for 5G networks," 12th European Conference on Antennas and Propagation (EuCAP 2018), London, 2018.
6. P. Tang, J. Zhang, A. F. Molisch, P. J. Smith, M. Shafi and L. Tian, "Estimation of the K-Factor for Temporal Fading From Single-Snapshot Wideband Measurements," in IEEE Transactions on Vehicular Technology, vol. 68, no. 1, pp. 49-63, Jan. 2019.